

Disturbance Estimation and Compensation in Exoskeleton Electric Drive Control with Neural Network

Dinh Dang Truong
 Department of Robotics and Industrial
 Automation
 Saint Petersburg Electrotechnical
 University "LETI"
 St. Petersburg, Russia
 dinhdangtruong@gmail.com

Mikhail P. Belov
 Department of Robotics and Industrial
 Automation
 Saint Petersburg Electrotechnical
 University "LETI"
 St. Petersburg, Russia
 milesa58@mail.ru

Pham Van Tuan
 Le Quy Don Technical University
 Hanoi, Vietnam
 tuanhvhq@gmail.com

Abstract—The article proposes a method to evaluate and compensate uncertain disturbance in exoskeleton electric drive control system. The mathematical model for exoskeleton electric drive system with taking into account the nonlinear components and the interaction force between exoskeleton and lower extremities is developed. The PD control combined with the RBF adaptive neural network is investigated with linear-quadratic regulator as the basic foundation of the feedback design to evaluate and compensate the unknown disturbances in control system. The PD ingredient is applied to stabilize the dominant model. The simulation results in Matlab/Simulink indicate that the proposed PD-linear quadratic regulator with adaptive neural network compensation is more efficiency in compared with the conventional PD-linear quadratic regulator.

Keywords—Exoskeleton; electric drive; control system; disturbance estimation; disturbance compensation; neural network.

I. INTRODUCTION

The exoskeleton electric drive control system is a complex system that requires high precision to ensure the stable movement of patients. The complexity of such systems due to the presence of elastic mechanical links. In the transient process, these links oscillate by themselves, which ultimately leads to complete instability of the operation of the exoskeleton electric drives. For a system including an exoskeleton and its wearer, there is no assurance that conventional regulators will provide the expected performance under external disturbances. Thus, it is a necessary real problem to the creation of reliable controllers in case of taking into account all of nonlinearities and disturbances. Several

methods of controlling the exoskeleton and its wearer were proposed based on the preliminary determination of the dynamic parameters [1], [2]. This method can be effective when the exoskeleton is worn by the same people in the same environments. Other approaches considered universal exoskeletons with the adaptive control which can be worn by people of different morphology [3], [4]. Several works on nonlinear control of exoskeletons were found in [5], [6].

II. MATHEMATICAL MODEL OF THE EXOSKELETON ELECTRIC DRIVES SYSTEM

The electric driver system of the exoskeleton hip and knee joints has the same design. Therefore, we will consider a physical model of the hip joint of an exoskeleton electric drive system as shown in Fig. 1 [7], where the driving motor is a brushless DC motor with parameters: v_a , i_a —phase voltage and current on the phase winding a stator respectively; R_a, L_a —resistor and inductance of the stator phase winding, respectively; M_m —torque on the engine shaft; θ_m —rotor angular position; J_m —rotor moment of inertia; M_f —frictional torque; J_g —inertia torque of gear; r_g —gear ratio; θ_g —angular position of the gearbox output shaft; k_g, k_s —rigidity; d_g, d_s —damping; θ_s —angular position of the spur gear;

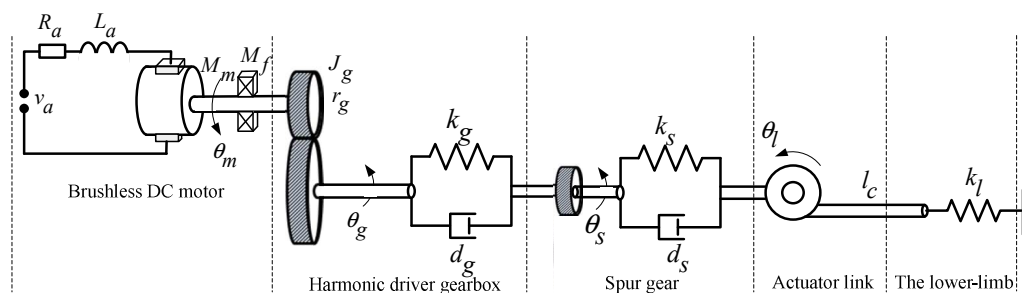


Fig. 1. Block diagram of the exoskeleton electric drives system

l_c —rigid connection between the torque sensor and the human lower limb; force interaction between the exoskeleton and the lower limb, which is modeled as a spring with stiffness k_f ; θ_l —angular position of the lower-limb.

The mathematical model of the system is built by a vector-matrix as follows:

$$\begin{cases} \dot{x}_1 = -\frac{R_a}{L_a}x_1 - \frac{R_a k_v}{L_a}x_3 + \frac{1}{L_a}v_a \\ \dot{x}_2 = x_3 \\ \dot{x}_3 = \frac{k_t}{J_m + J_g}x_1 - \frac{d_g + k_g}{r_g^2(J_m + J_g)}x_2 + \frac{k_g}{r_g(J_m + J_g)}x_4 \\ \quad + \frac{d_g}{r_g(J_m + J_g)}x_5 - \frac{1}{J_m + J_g}M_f \\ \dot{x}_4 = x_5 \\ \dot{x}_5 = \frac{d_g + k_g}{J_s r_g}x_2 - \frac{k_g + k_s}{J_s}x_4 - \frac{d_g}{J_s}x_5 + \frac{k_s}{J_s}x_6 \\ \dot{x}_6 = \frac{k_s}{k_f l_c}x_4 + \frac{d_s}{k_f l_c}x_5 - \frac{d_s}{k_f l_c} \left(\frac{k_s}{d_s} + 1 \right) x_6 \end{cases}$$

The mathematical model of the system is described by a vector-matrix as follows:

$$\begin{cases} \dot{\mathbf{x}} = \mathbf{A}\mathbf{x} + \mathbf{B}\mathbf{u} + \mathbf{B}_d \mathbf{F}(\mathbf{x}, u) + \mathbf{d} \\ \mathbf{y} = \mathbf{C}\mathbf{x} \end{cases} \quad (1)$$

where $\mathbf{x} = [x_1 \ x_2 \ x_3 \ x_4 \ x_5 \ x_6]^T$ —vector of state variables: $x_1 = i_a$, $x_2 = \theta_m$, $x_3 = \dot{\theta}_m$, $x_4 = \theta_s$, $x_5 = \dot{\theta}_s$,

$x_6 = \theta_j$; $\mathbf{A} \in R^{6 \times 6}$ —matrix of states;

$\mathbf{B} = \begin{bmatrix} 1/L_a & 0 & 0 & 0 & 0 & 0 \end{bmatrix}^T$ —control matrix;

$\mathbf{B}_d = \begin{bmatrix} 0 & 0 & -1/(J_m + J_g) & 0 & 0 & 0 \end{bmatrix}^T$ —disturbances matrix;

$\mathbf{C} = \begin{bmatrix} 0 & 0 & 0 & 0 & 0 & 1 \end{bmatrix}$ —output matrix;

$\mathbf{F}(\mathbf{x}, u) = \begin{bmatrix} 0 & 0 & f(\mathbf{x}, u) & 0 & 0 & 0 \end{bmatrix}^T$ —vector of a nonlinear function, where the mathematical expression for calculating friction that takes the form [8]:

$$f(\mathbf{x}, u) = \alpha_1 \tanh(\alpha_2 x_3) + \alpha_3 x_3,$$

where $\alpha_i \in \mathbb{R}^+$, $\forall i = 1, 2, 3$ —unknown positive constants;

$\mathbf{d} = [0 \ 0 \ d(t) \ 0 \ 0 \ 0]^T$ —matrix of slowly changing external disturbances that cannot be measured and blocked $|d(t)| < d_m$.

III. CONTROL SYSTEM SYNTHESIS

In this section, we propose a control method consisting of PD and adaptive RBF (Radial Basis Function) compensator for the disturbances. A linear quadratic regulator (LQR) is used as the basic foundation of the feedback design with estimation and compensation of the disturbance by neural network (NN) for purpose of synthesizing the exoskeleton electric drive control system. The block diagram of the control system is shown in Fig. 2.

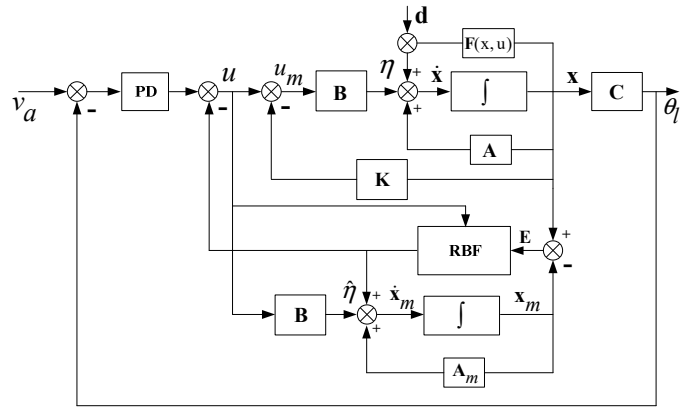


Fig. 2. The block diagram of the control system

The optimal control using LQR synthesis with the function of quality indicators is given as:

$$J = \frac{1}{2} \int_0^{\infty} [\mathbf{x}^T \mathbf{Q} \mathbf{x} + \mathbf{u}^T \mathbf{R} \mathbf{u}] dt$$

where \mathbf{Q} —weighted symmetric diagonal matrix expressing the tracking mismatch between the actual and the specified desired behavior of the control object ($\mathbf{Q} \geq 0$); \mathbf{R} —weighted symmetric diagonal matrix reflecting an abrupt change in control actions ($\mathbf{R} > 0$). The negative feedback matrix \mathbf{K} is defined corresponding to the LQR control method.

In this study, the RBF neural network is used to perform synthesis, evaluate and compensate the undefined disturbance. With the feedback matrix, the kinematics of the control system (1) can be written as:

$$\dot{\mathbf{x}} = \mathbf{A}_m \mathbf{x} + \mathbf{B}\mathbf{u} + \mathbf{B}_d \mathbf{F}'(\mathbf{x}, u) + \mathbf{d} \quad (2)$$

where $\mathbf{A}_m = \mathbf{A} - \mathbf{K}$, $\mathbf{F}'(\mathbf{x}, u) = [0, \dots, f(\mathbf{x}, u), 0, \dots]^T$

The nonlinearity and perturbation elements (2) are estimated by:

$$\dot{\mathbf{x}}_m = \mathbf{A}_m \mathbf{x}_m + \mathbf{B}\mathbf{u} + \mathbf{B}_d \hat{\mathbf{F}}(\mathbf{x}, u) + \hat{\mathbf{d}} \quad (3)$$

where \mathbf{x}_m —state vector of evaluation model;

$$\hat{\mathbf{F}}(x, u) = [0, \dots, \hat{f}(x, u), \dots]^T \text{ —nonlinear function estimation}$$

vector of $\mathbf{F}'(x, u)$; $\hat{\mathbf{d}} = [0, \dots, \hat{d}(t), \dots]^T$ —evaluation vector \mathbf{d} .

If $\mathbf{F}'(x, u)$ can be determined through the evaluation function $\hat{\mathbf{F}}(x, u_m)$, \mathbf{d} through $\hat{\mathbf{d}}$ so that:

$$|\mathbf{F}'(x, u) - \hat{\mathbf{F}}(x, u)| \leq \varepsilon_1, \varepsilon_1 = [0, \dots, \eta_1, \dots]^T$$

where η_1, η_2 are arbitrarily small, then the nonlinear element and the disturbance are compensated as shown in Fig. 2, and hence a linear element and an error remain $\varepsilon_1, \varepsilon_2$ in (2). Eq. (2) and Eq. (3) can be rewritten as follows:

$$\dot{\mathbf{E}} = \mathbf{A}_m \mathbf{E} + \tilde{\mathbf{F}} + \tilde{\mathbf{d}} \quad (4)$$

where $\mathbf{E} = \mathbf{x} - \mathbf{x}_m$;

$$\tilde{\mathbf{F}} = \mathbf{F}'(x, u) - \hat{\mathbf{F}}(x, u) \quad (5)$$

$$\tilde{\mathbf{d}} = \mathbf{d} - \hat{\mathbf{d}}$$

Since the vector of the function $\mathbf{F}'(x, u)$ is smooth, therefore for the approximation, we use the RBF neural network with 3 layers (7 input layer neurons, 10 hidden layer neurons, 1 output layer neuron) [9]. The structure of the RBF neural network is shown in Fig. 3.

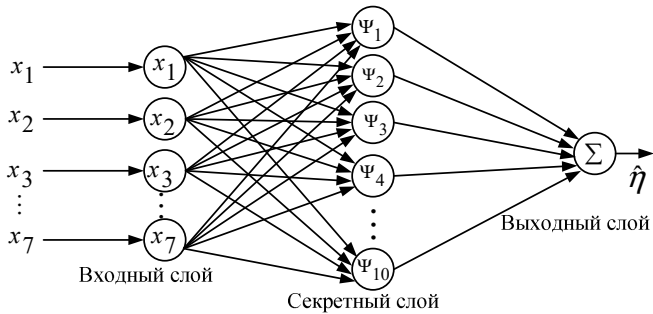


Fig. 3. The structure of the RBF neural network

$\mathbf{F}'(x, u)$ is presented via a base function $\Psi_i(\bar{\mathbf{x}})$, where $\bar{\mathbf{x}} = [x_1 \dots x_6, u]^T$ then:

$$\mathbf{F}'(x, u) = \mathbf{F}'(\bar{\mathbf{x}}) = \left[0, \dots, \sum_{i=1}^m W_i \Psi_i(\bar{\mathbf{x}}), \dots \right]^T + \varepsilon_1 \quad (6)$$

where $W_i, i = 1, 2, \dots, m$ —weight with a sufficient number of basic functions to ensure a given approximate error.

Basic functions $\Psi_i(\bar{\mathbf{x}})$ are selected as follows:

$$\Psi_i(\bar{\mathbf{x}}) = \exp \left(-\frac{\|\bar{\mathbf{x}} - c_i\|^2}{2\sigma^2} \right) / \sum_{i=1}^m \exp \left(-\frac{\|\bar{\mathbf{x}} - c_i\|^2}{2\sigma^2} \right) \quad (7)$$

where c_i is two-dimensional vector representing the center of the i^{th} basis function, and σ is the variance representing the spread of the basis function [10].

Evaluation vector $\hat{\mathbf{F}}(x, u_m)$ is expressed as a basis function (7) with the corrects weight \hat{W}_i .

$$\hat{\mathbf{F}}(x, u) = \hat{\mathbf{F}}(\bar{\mathbf{x}}) = [0, \dots, \hat{f}(\bar{\mathbf{x}}), \dots]^T = \left[0, \dots, \sum_{i=1}^m \hat{W}_i \Psi_i(\bar{\mathbf{x}}), \dots \right]^T \quad (8)$$

The neural network training process is the process of adjusting weight, \hat{W}_i , of the RBF neural network output layer with the weight difference.

$$\tilde{W}_i = W_i - \hat{W}_i \quad (9)$$

Transforming (6) and (8), we obtain:

$$\mathbf{F}'(\bar{\mathbf{x}}) = \hat{\mathbf{F}}(\bar{\mathbf{x}}) + \varepsilon^*$$

where $\varepsilon^* = \varepsilon_1 - \left[0, \dots, \sum_{i=1}^m \tilde{W}_i \Psi_i(\bar{\mathbf{x}}), \dots \right]^T$; $\varepsilon^* = \varepsilon_1$ when the $\tilde{W}_i \rightarrow 0, i = 1, 2, \dots, m$.

The Lyapunov function is applied for the system (4) as follows:

$$V = \mathbf{E}^T \mathbf{P} \mathbf{E} + \sum_{i=1}^m \tilde{W}_i^2 + \tilde{\mathbf{d}}^2 \quad (10)$$

where \mathbf{P} —positive definite symmetric matrix.

Theorem. For the stability of system (4), the following conditions must be simultaneously satisfied:

$$\|\mathbf{E}\| > \frac{2\eta_1 \|\bar{\mathbf{P}}_n\|}{\gamma_1}; \quad (11)$$

$$\dot{\tilde{W}}_i = -\bar{\mathbf{P}}_n \mathbf{E} \Psi_i(\bar{\mathbf{x}}); \quad (12)$$

$$\dot{\tilde{\mathbf{d}}} = -\bar{\mathbf{P}}_n \mathbf{E}; \quad (13)$$

$$k_{n-1} = (-1)^{n-1} (-1)^{n-1} c_{n-1} - a_{n-1}; \quad (14)$$

IV. SIMULATION RESULTS.

The parameters of electric driver system are shown in Table 1.

TABLE 1. THE PARAMETERS OF ELECTRIC DRIVER SYSTEM

Параметры	Знач	Параметры	Знач	Параметры	Знач
R_a, Ω	0.522	$J_g, \text{kg.m}^2$	$2.82 \cdot 10^{-2}$	$k_g, \text{Nm/rad}$	270
L_a, mH	0.625	$d_g, \text{Nm.s/rad}$	2.09	l_c, m	0.313
$k_l, \text{m.Nm/A}$	109	$k_s, \text{Nm/rad}$	81.853	α_1	0
$k_v, \text{rpm/V}$	88	$J_s, \text{kg.m}^2$	$0.48 \cdot 10^{-3}$	α_2	100
$J_m, \text{kg.m}^2$	$0.3 \cdot 10^{-2}$	$d_s, \text{Nm.s/rad}$	$0.74 \cdot 10^{-3}$	α_3	0.01
r_g	160	$k_l, \text{N/m}$	97		

The exoskeleton has constantly confronted with external disturbances and model uncertainties as various heights, masses, and disease states such as varying degrees of spasticity. Therefore, a random perturbation is used to check the stability of the proposed control method to external disturbances and model uncertainties. The electric driver control system of the exoskeleton is modeled in the Matlab/Simulink with an external disturbance [11]: $d(t) = 0.5 * \text{randn}(1, 1)$; The covariance matrices to calculate the optimal negative feedback matrix of the LQR control: $\mathbf{R} = [0.015]$; $\mathbf{Q} = \text{diag}(50, 50, 50, 50, 50, 100)$; The gain coefficients of the PD controller: $K_P = 52.5$; $K_D = 78$; The training methods of Bayesian Regularization (*trainbr*) of back propagation.

In Fig. 4-6 show the results of simulation in the Matlab/Simulink environment.

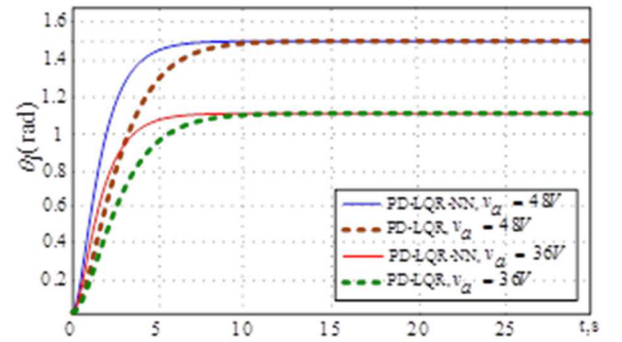


Fig 4. Angular position response of the lower-limb θ

$$k_n = (-1)^n (-1)^n c_n - a_n \quad (15)$$

where $\bar{\mathbf{P}}_n$ —row matrix is formed from the n -th row of the matrix \mathbf{P} ; γ_1 —minimum eigenvalue of the matrix

$$\mathbf{Q} = -\left[\mathbf{A}_m^T \mathbf{P} + \mathbf{P} \mathbf{A}_m \right];$$

$$(-1)^{n-1} c_{n-1} = \lambda_1 \lambda_2 \dots \lambda_{n-1} + \lambda_1 \lambda_2 \dots \lambda_{n-2} \lambda_n + \dots + \lambda_2 \lambda_3 \dots \lambda_n$$

; $(-1)^n c_n = \lambda_1 \lambda_2 \dots \lambda_{n-1} \lambda_n$ (λ_i —solution of the characteristic equation of the system).

Expressions in (12), (13) of the theorem represent the law of estimation for nonlinear elements and perturbations. Substituting (12) in (9) we can get:

$$\dot{W}_i - \hat{W}_i = -\bar{\mathbf{P}}_n \mathbf{E} \Psi_i(\bar{\mathbf{x}}) \quad (16)$$

Because $W_i = \text{const} \rightarrow \dot{W}_i = 0$ then:

$$\hat{W}_i = \bar{\mathbf{P}}_n \mathbf{E} \Psi_i(\bar{\mathbf{x}}) \quad (17)$$

By integrating equation (17), we obtain the law of weight renewal:

$$\hat{W}_i = \int \bar{\mathbf{P}}_n \mathbf{E} \Psi_i(\bar{\mathbf{x}}) d(t) \quad (18)$$

Substituting (18) in (8), we obtain the law of the indefinite vector $\mathbf{F}'(\mathbf{x}, \mathbf{u})$ through $\hat{\mathbf{F}}(\bar{\mathbf{x}}) = [0, \dots, \hat{f}(\bar{\mathbf{x}}), \dots]^T$.

$$\hat{f}(\bar{\mathbf{x}}) = \sum_{i=1}^m \int (\bar{\mathbf{P}}_n \mathbf{E} \Psi_i(\bar{\mathbf{x}})) d(t) \times \Psi_i(\bar{\mathbf{x}}) \quad (19)$$

Substituting (13) in (5) we get:

$$\dot{\mathbf{d}} - \hat{\mathbf{d}} = -\bar{\mathbf{P}}_n \mathbf{E}$$

Due to slowly change of \mathbf{d} , we get:

$$\hat{\mathbf{d}} = -\bar{\mathbf{P}}_n \mathbf{E} \quad (20)$$

Integrating (20), we obtain the disturbance estimation law:

$$\hat{\mathbf{d}} = \int \bar{\mathbf{P}}_n \mathbf{E} d(t) \quad (21)$$

From expressions in (19) and (21), we obtain the estimation law to compensate for indefinite nonlinear elements and external disturbances (22).

$$\hat{\eta} = \sum_{i=1}^m \int (\bar{\mathbf{P}}_n \mathbf{E} \Psi_i(\bar{\mathbf{x}})) dt \times \Psi_i(\bar{\mathbf{x}}) + \int \bar{\mathbf{P}}_n \mathbf{E} dt \quad (22)$$

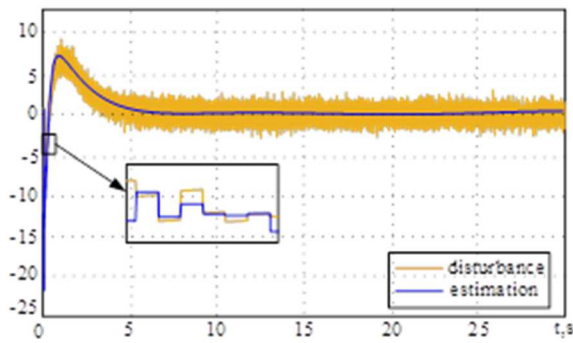


Fig 5. Neural network that identifies disturbance $\hat{\eta}$

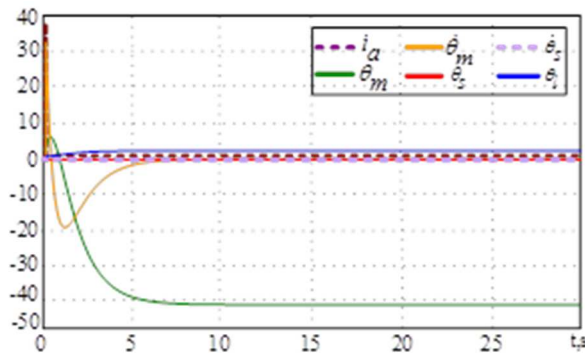


Fig 6. Stabilizes the system state vectors

V. CONCLUSION.

The paper proposes a method for identifying undefined nonlinear elements and external disturbances for the electric drive control system of the exoskeleton. The advantage of this method is to pass from an unstable nonlinear problem to a linear problem with the additional negative feedbacks. Using powerful neural network tools leads to the law of estimation of a nonlinear function of uncertain external disturbances. The estimation and calibration process occurs once the nonlinear element and external disturbance change, which does not depend on any other factors. The quadratic model is used as

the basic foundation of the feedback design, and an adaptive ingredient designed based on a RBF produces for the possibility of performance enhancement when the feedback control alone is inadequate. The simulation results demonstrate the effectiveness of the proposed method.

REFERENCES

- [1] J. Ghan, R. StegerandH. Kazerooni. "Control and system identification for the Berkeley lower extremity exoskeleton (BLEEX)", *Advanced Robotics*, Vol. 20, No. 9, pp. 989-1014. 2006.
- [2] Ghan J., Kazerooni H. "System identification for the Berkeley lower extremity exoskeleton (BLEEX)" //*Proceedings 2006 IEEE International Conference on Robotics and Automation, 2006. ICRA 2006.* – IEEE, 2006. – C. 3477-3484.
- [3] H. B. Kang and J. H. Wang, "Adaptive control of 5 DOF upper-limb exoskeleton robot with improved safety", *ISA Trans.* Vol. 52, No. 6, pp. 844-852, 2013.
- [4] Madani T., Daachi B., Djouani K. "Adaptive controller based on uncertainty parametric estimation using backstepping and sliding mode techniques: application to an active orthosis" //*2014 European Control Conference (ECC).* – IEEE, 2014. – C. 1869-1874.
- [5] Madani T., Daachi B., Djouani K. "Finite-time control of an actuated orthosis using fast terminal sliding mode" //*IFAC proceedings volumes.* – 2014. – T. 47. – №. 3. – C. 4607-4612.
- [6] S. Balasubramanian and J. He, "Adaptive control of a wearable exoskeleton for upper extremity neurorehabilitation", *Applied Bionics and Biomechanics*, Vol. 9, No. 1, pp. 99-115, 2012
- [7] Barjuei E. S. et al. "Bond graph modeling of an exoskeleton actuator" //*2018 10th Computer Science and Electronic Engineering (CEECE).* – IEEE, 2018. – C. 101-106.
- [8] Makkar C. et al. "A new continuously differentiable friction model for control systems design" //*Proceedings, 2005 IEEE/ASME International Conference on Advanced Intelligent Mechatronics.* – IEEE, 2005. – C. 600-605.
- [9] Belov M. P., Khoa T. D., Truong D. D. "Blde of robotic manipulators with neural torque compensator based optimal robust control" //*2019 IEEE Conference of Russian Young Researchers in Electrical and Electronic Engineering (EIConRus).* – IEEE, 2019. – C. 437-441.
- [10] Huang S. N., Tan K. K., Lee T. H. "A combined PID/adaptive controller for a class of nonlinear systems" //*Automatica.* – 2001. – T. 37. – №. 4. – C. 611-618.
- [11] Rahmani M., Rahman M. H. "Novel robust control of a 7-DOF exoskeleton robot" //*PloS one.* – 2018. – T. 13. – №. 9. – C. e0203440.